MAJOR ARTICLE

Disrupted Anabolic and Catabolic Processes May Contribute to Alcohol-Accentuated SAIDS-Associated Wasting

Nicole J. LeCapitaine,[1,2] Zhong Q. Wang,[3] Jason P. Dufour,[4] Barry J. Potter,[1] Gregory J. Bagby,[1,2] Steve Nelson,[2,5] William T. Cefalu,[3] and Patricia E. Molina[1,2]

[1]Department of Physiology, and [2]Comprehensive Alcohol Research Center, Louisiana State University, Health Sciences Center, New Orleans; [3]Joint Program on Diabetes, Endocrinology, and Metabolism, Pennington Biomedical Research Center, Baton Rouge, and Louisiana State University, Health Sciences Center, New Orleans; [4]Division of Veterinary Medicine, Tulane National Primate Research Center, Covington; and [5]School of Medicine, Louisiana State University, Health Sciences Center, New Orleans, Louisiana

Background. Alcohol abuse is a comorbid factor in many human immunodeficiency virus (HIV)–infected patients. Previously, we demonstrated that chronic binge alcohol accentuates loss of body mass at terminal stage of simian immunodeficiency virus (SIV) infection. The purpose of this study was to investigate changes in pathways that may contribute to muscle wasting in chronic binge alcohol-fed SIV-infected macaques.

Methods. The impact of chronic binge alcohol during SIV infection on insulin signaling and the ubiquitin (Ub)–proteasome system—regulators of protein synthesis and degradation—was examined in SIV-infected macaques.

Results. SIV infection induced an inflammatory and pro-oxidative milieu in skeletal muscle, which was associated with decreased insulin-stimulated phosphatidylinositol 3-kinase (PI-3k) activity and upregulated gene expression of *mTOR* and *atrogin-1*, and protein expression of Ub-proteasome system 19S base. Chronic binge alcohol accentuated the skeletal muscle pro-oxidative milieu and 19S base expression. Additionally, chronic binge alcohol increased skeletal muscle protein expression of protein-tyrosine phosphatase 1B (a negative regulator of insulin signaling) and 19S proteasome regulator non-ATPase (Rpn) 6 subunit and Rpn12, and suppressed PI-3K activity. Animals that were alcohol-fed and SIV-infected for >15 months had increased Ub-proteasome system activity.

Conclusions. These data suggest negative modulation of insulin signaling coupled with enhanced Ub-proteasome system activity may be central mechanisms underlying chronic binge alcohol-induced accentuation of SIV-associated muscle wasting.

According to the Centers for Disease Control and Prevention, >400 000 people were living with AIDS in the United States at the end of 2003 [1]. The reduction in human immunodeficiency virus (HIV)–associated morbidity and mortality resulting from the use of highly active antiretroviral therapy (HAART) has made HIV infection a chronic disease, during which individuals are likely to engage in alcohol and drug abuse at rates comparable to those in the noninfected population [2]. Chronic alcohol consumption remains the most common and costly form of drug abuse with ~14 million Americans fulfilling the diagnostic criteria for alcohol abuse and/or alcoholism. Indeed, alcohol abuse and HIV infection frequently co-exist [3].

Muscle wasting remains an important determinant of increased morbidity and mortality observed in AIDS [4–7]. Chronic alcohol abuse is associated with skeletal muscle myopathy [8] resulting from decreased muscle protein synthesis [9–11] and possibly accelerated muscle

Received 20 January 2011; accepted 1 June 2011.

Presented in part: 10th Annual Meeting of Research Society on Alcoholism, Austin, TX, June 2010. Abstract 328; Alcohol Research Interest Group, Chicago, IL, November 2010.

Correspondence: Patricia E. Molina, MD, PhD, Department of Physiology, LSUHSC, 1901 Perdido St, New Orleans, LA 70112 (pmolin@lsuhsc.edu).

The Journal of Infectious Diseases 2011;204:1246–55

0022-1899 (print)/1537-6613 (online)/2011/2048-0014$14.00
DOI: 10.1093/infdis/jir508

proteolysis [12]. Additionally, indirect effects of alcohol such as alterations in nutritional state, micronutrient availability, and growth factor expression have been implicated in the etiology of alcohol-induced muscle wasting [13]. Because loss of lean body mass has a deleterious impact on the overall survival of HIV-infected individuals, factors that accelerate this process, such as chronic alcohol consumption, likely accelerate disease progression and development of AIDS-associated wasting [14–17]. We have previously shown that chronic binge alcohol-administered SIV-infected (ALC/SIV$^+$) macaques had significantly lower body weight, body mass index (BMI), and limb muscle area compared with sucrose-treated SIV-infected (SUC/SIV$^+$) animals [18]. In addition, our studies showed messenger RNA (mRNA) expression of *IGF-1* is suppressed, *atrogin-1* is increased, *TNF-α* is significantly increased, and *myostatin* is modestly elevated in skeletal muscle from ALC/SIV$^+$ animals at terminal stage of SIV infection (SAIDS) [18]. Atrogin-1 is a muscle-specific E3 ubiquitin ligase and has been implicated as a causal factor in muscle wasting [19]. Tumor necrosis factor α (TNF-α) has been shown to exert anti-insulin effects in skeletal muscle [20, 21], and the negative regulator of skeletal muscle growth, myostatin [22], has been implicated in muscle wasting in HIV-infected men [23]. Together, our findings suggested upregulation of the ubiquitin (Ub)–proteasome system as a predominant mechanism underlying loss of skeletal muscle mass observed in those studies. However, it was not investigated whether parallel suppression in anabolic regulatory pathways was also involved. Moreover, whether localized skeletal muscle inflammation was associated with an oxidative milieu further contributing to dysregulation in muscle mass was not investigated. The present study extends our observations to integrate the role of disrupted anabolic signaling as an additional, potentially synergistic mechanism that is responsible for disruption in the balance between the synthetic and catabolic mechanisms leading to erosion of muscle mass in chronic binge alcohol-administered SIV-infected macaques.

MATERIALS AND METHODS

All experiments were approved by the Institutional Animal Care and Use Committee at both Tulane National Primate Research Center (TNPRC) in Covington, Louisiana, and Louisiana State University Health Sciences Center in New Orleans, Louisiana, and adhered to National Institutes of Health guidelines for the care and use of experimental animals. Four- to six-year-old male macaques (*Macaca mulatta*) obtained from TNPRC breeding colonies were studied. Excellent health of animals was determined by (1) complete physical examinations by a veterinarian; (2) complete blood counts and serum chemistries; and (3) negative serological status for simian retrovirus (confirmed by DNA amplification by nested polymerase chain reaction [PCR], enzyme immunoassay [EIA], and Western immunoblot analysis) and simian T-lymphotropic virus type 1 (EIA and Western immunoblot analysis) based on assays performed by the Pathogen Detection Laboratory (California National Primate Research Center, Davis, CA). Age- and body-weight-matched animals were randomized to either isocaloric SUC/SIV$^+$ or ALC/SIV$^+$ groups. Skeletal muscle samples were obtained at necropsy from a group of SIV-negative, healthy control macaques (age, 7.4 ± 1.10 years; weight [mean +/- SEM], 11.1 ± 1.51 kg) and used as reference values for comparison of analyzed variables. A total of 28 animals were studied: 9 in the SUC/SIV$^+$ group, 11 in the ALC/SIV$^+$ group, and 8 in the control group. Animals were individually housed in a Biosafety Level 2 containment building.

Experimental Protocol

The gastric catheter placement for alcohol delivery, the alcohol delivery protocol, and the route of SIV infection have been described elsewhere [18, 24]. Animals were exposed to chronic alcohol by intragastric administration of a mean of 13–14 grams of ethanol (30% w/v water) per kilogram of body weight per week beginning 3 months prior to SIV infection and continued throughout the duration of study. This approach of intragastric delivery was selected to reduce experimental variability and ensure chronic binge-like intoxicating blood alcohol concentrations of 50–60 mmol/L. Total calories provided by alcohol and sucrose averaged 15%. Animals were provided monkey chow ad libitum (Lab Fiber Plus Primate diet DT; PMI Nutrition International, St. Louis, MO) and supplemented with fruits, vitamins, and Noyes treats (Research Diets, New Brunswick, NJ).

Three months after initiating chronic binge alcohol administration, animals were inoculated intravenously with 10,000 times the 50% infective dose (ID_{50}) of SIV_{mac251}, provided by Preston Marx. Intravenous inoculation was performed at the conclusion of an ethanol or sucrose session when blood alcohol levels were elevated to simulate infection during an alcohol binge. The progression of SIV disease was monitored throughout the study period through clinical, biochemical, and immunological parameters (CD4/CD8 lymphocyte ratios) in addition to plasma viral kinetics (SIV *gag* RNA levels) as described elsewhere [18, 24, 25]. Skeletal muscle (gastrocnemius) samples were obtained at necropsy when animals met criteria for euthanasia based on the following: (1) loss of 25% of body weight from maximum body weight since assignment to protocol; (2) major organ failure or medical conditions unresponsive to treatment; (3) surgical complications unresponsive to immediate intervention; or (4) complete anorexia for 4 days. Because of the large range in time of SIV infection within the groups, initial data analyses grouped results based on time after SIV infection, as either early infection or late infection. The late infection group is defined as the group with time to euthanasia that was ≥2 SD from the mean time to euthanasia in the early infection group. In the SUC/SIV$^+$ group, the mean time (± SD) of SIV infection for the early

(n = 6) and late (n = 3) infection groups was 5.2 ± 2.3 months and 24.3 ± 8.2 months, respectively. In the ALC/SIV$^+$ group, the mean time (± SD) of SIV infection for the early (n = 8) and late (n = 3) infection groups was 5.3 ± 3.0 months and 25.4 ± 5.9 months, respectively. No significant differences were found in outcome measures obtained in these animals on analysis according to early or late infection, with the exception of proteasome activity. Thus, with the exception of proteasome activity, for which both combined and late infection values are shown, results represent the combined data of both early and late subgroups. In addition, no significant differences were noted in viral load (~6.3 log copies/mL) or CD4/CD8 cell ratio (~0.7) at time of necropsy, as reported elsewhere [18].

Muscle mRNA and Protein Expression

Muscle samples were frozen in liquid nitrogen and stored at −80°C until analyses. Samples were homogenized and total RNA was isolated using an RNeasy Mini kit (Qiagen, Valencia, CA) according to the manufacturer's instructions. Muscle tissue lysates were dissected and homogenized using a PRO 200 homogenizer (PRO scientific, Oxford, CT) in buffer A (25 mmol/L HEPES [pH, 7.4], 1% Nonidet P-40 [NP-40], 137 mmol/L NaCl, 1 mmol/L PMSF, 10 μg/mL aprotinin, 1 μg/mL pepstatin, and 5 μg/mL leupeptin). Samples were centrifuged at 14 000 *g* for 20 minutes at 4°C, and protein concentrations were determined by a BCA protein assay kit (Bio-Rad Laboratories, Hercules, CA).

Real-time Reverse-Transcription PCR Primers and Probes

The amplification primers and probes used for determination of *TNF-α, IFN-γ, IL-6, IL-1β,* and *atrogin-1* were purchased from Applied Biosystems (Carlsbad, CA) and used according to the manufacturer's instructions. The amplification primers and FAM-labeled probes used for determination of *RPS13* and *mTOR* are as follows: RPS13 forward primer, 5′- TCTGACGACGTGAAGGAGCAGATT; RPS13 reverse primer, 5′-TCTCTCAGGATCACACCGATTTGT; RPS13 probe, 5′-AAACTGGCCAAGAAGGGCCTGACTCCTT; mTOR forward primer, 5′-AGTGTCTTGCTCTGTTGTCAGGCT; mTOR reverse primer, 5′-AAATTAGCTGGGCATGGTGGTGC; mTOR probe, 5′-AAGCAATTCTCCTGCCTCAGCCTCCCAA.

Real-time Quantitative Reverse-Transcription PCR

Total RNA was reverse transcribed and real-time PCR was performed with a Superscipt III Platinum 2-step quantitative reverse-transcription PCR (RT-qPCR) kit according to the manufacturer's instructions (Invitrogen, Carlsbad, CA). All reactions were performed on a CFX96 system (Bio-Rad Laboratories, Hercules, CA). The primer and probe concentrations were 500 and 150 nmol/L, respectively, for *RPS13* and *mTOR,* respectively, and RT-qPCR data were analyzed using the $\Delta\Delta C_T$ method. Target genes were compared with the endogenous control, *RPS13,* and normalized to control values or to SUC/SIV$^+$ values if the target was not detectable in control samples. *RPS13* was chosen as the endogenous control based on a meta-analysis of 13 629 human gene array samples to determine the most stably expressed genes [26].

Western Blot Analysis

Muscle proteins (50 μg) were resolved by sodium dodecyl sulfate polyacrylamide gel electrophoresis and subjected to immunoblot analysis. Protein abundance was detected with antibodies against insulin receptor substrate 1 (IRS-1), IRS-2, phosphatidylinositol 3 kinase (PI3-K), Akt1, Akt2, protein-tyrosine phosphatase 1B (PTP1B), and 19S base S5A subunit (Upstate, Lake Placid, NY); insulin receptor β subunit (IRβ; Santa Cruz Biotechnology, Santa Cruz, CA); glucose transporter type 4 (GLUT4; R&D Systems, Minneapolis, MN); 19S proteasome regulator non-ATPase 6 subunit (Rpn6) and Rpn12 (Biomol International, Plymouth Meeting, PA); and β-actin (Sigma-Aldrich, St. Louis, MO), using Chemiluminescence Reagent Plus (PerkinElmer Life Science, Boston, MA), and quantified with a densitometer. Proteins were normalized to β-actin.

Ex Vivo Antioxidant Capacity Determinations

Antioxidant capacity was determined in skeletal muscle homogenates according to the method of Klemm et al [27]. Briefly, snap-frozen samples of tissue were pneumatically homogenized and mixed with Dulbecco phosphate-buffered saline containing 3.5 mmol/L glucose (pH, 7.4; concentration, 1:10) on ice. The samples were incubated (shaking water bath at 37°C) in the presence or absence of 10 mmol/L *N*-ethylmaleimide (to prevent glutathione recycling) for 30 minutes. At time 0, CPH (1-hydroxy-3-carboxy-2,2,5,5-tetramethylpyrrolidine HCl) and tertiary butyl hydroperoxide were added to the samples at final concentrations of 2.0 and 0.4 mmol/L, respectively, and the mixture was incubated in the shaking water bath for 30 minutes. The samples were then snap-frozen and stored in liquid nitrogen until X-band electron paramagnetic resonance (EPR) spectroscopy was performed. On analysis, samples were quickly thawed in a water bath at 37°C, aspirated into glass capillaries (ID, 0.8 mm), and read at room temperature using a Bruker EMX (Bruker BioSpin, Billerica, MA) with the following settings: microwave power, 40 mW; frequency, 9.79 GHz; center field, 3485 G; sweep width, 100 G; time constant, 10.3 milliseconds; sweep time, 10 seconds (5 sweeps); and receiver gain, 7.9×10^3. Scans from samples incubated in the absence of *N*-ethylmaleimide were subtracted from the corresponding ones in its presence with the derivative data subjected to double integration using WINEPR software (Bruker BioSpin, Billerica, MA); values are expressed as a percentage of antioxidant capacity.

PI3-K Activity Assay

IRS-1–associated PI3-K activity levels were assessed as described elsewhere [28, 29]. Briefly, 500 μg of muscle lysate was immunoprecipitated with 3 μg of IRS-1 antibody and protein

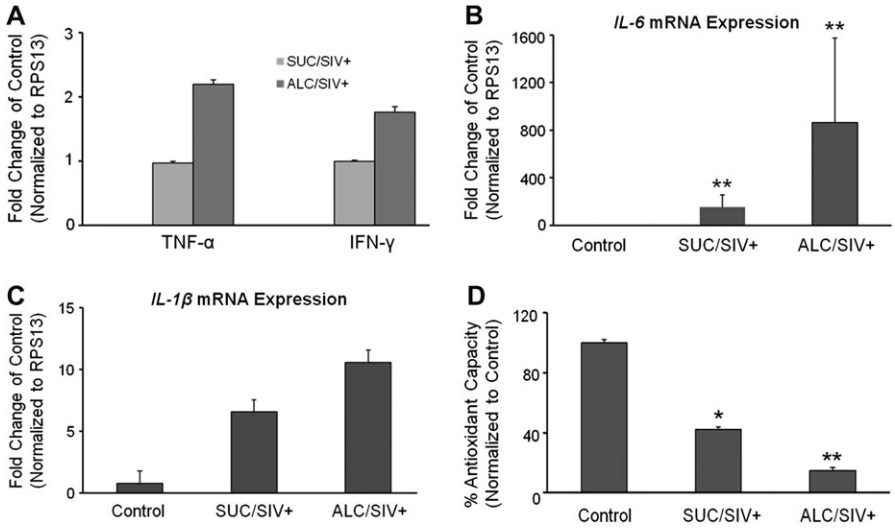

Figure 1. Skeletal muscle inflammatory and oxidative milieu. *A,* Tumor necrosis factor α gene (*TNF-α*) and interferon γ (*IFN-γ*) messenger RNA (mRNA) levels expressed as fold change of values in sucrose-treated simian immunodeficiency virus (SIV)–infected (SUC/SIV$^+$) rhesus macaques because they were not detected in control samples. *B, C,* Levels of interleukin 6 gene (*IL-6*) and interleukin 1β gene (*IL-1ß*) mRNA, respectively, expressed as fold change of values in control animals (n = 5) in skeletal muscle of SUC/SIV$^+$ animals (n = 9) and chronic binge alcohol-administered SIV-infected (ALC/SIV$^+$) animals (n = 10). *D,* Percentage of antioxidant capacity in skeletal muscle of control animals (n = 5), SUC/SIV$^+$ animals (n = 5), and ALC/SIV$^+$ animals (n = 5). *P* values were obtained by 1-way analysis of variance with a Kruskal-Wallis test followed by a Dunn multiple comparisons test. *$P < .05$ versus control; **$P < .01$ versus control.

A agarose. IRS immune complexes were incubated (10 minutes at 22°C) in 50 μL of 20 mmol/L Tris/HCl buffer (pH, 7.0) containing 50 μmol/L [[γ]-^{32}P] ATP (5 μCi; Perkin Elmer, Boston, MA), 10 mmol/L $MgCl_2$, 2 mmol/L $MnCl_2$, 100 mmol/L NaCl, 2 mmol/L EDTA, and 10 μg of phosphatidylinositol. After thin layer chromatography, radiolabeled phosphatidylinositol 3-phosphate was visualized by autoradiography and quantitated by densitometry (BioRad, Hercules, CA).

20S Proteasome Activity Assay

20S proteasome activity levels were measured using a 20S Proteasome Activity assay kit (Chemicon International, Temecula, CA) according to the manufacturer' s instructions. Briefly, 20 μg of muscle lysate was incubated (30 minutes at 37°C) with fluorophore 7-amino-4-methylcoumarin (AMC)–labeled specific 20S proteasome substrates LLVY-AMC. The free AMC fluorescence was quantified using a 380/460 nm filter set in a fluorometer (BioTex, Winooski, VT). The AMC standard curve was generated with a dilution series of purified 20S proteasome. Each sample/substrate combination was assayed in duplicate, both in the presence and in the absence of the proteasome inhibitor MG132 (20 μmol/L; Calbiochem, La Jolla, CA).

Data Analysis

All data are presented as the mean (± SEM) in each experimental group. The sample size is included in the legend of each figure. Treatment effects were established using 1-way analysis of variance with a Kruskal-Wallis test followed by a Dunn multiple comparisons test. Results for which $P \leq .05$ were considered to be statistically significant. Statistical analyses were performed using Prism 5 software (GraphPad Software, San Diego, CA).

RESULTS

SIV Infection and Chronic Binge Alcohol Consumption Favor Skeletal Muscle Inflammation and Oxidative Stress

Skeletal muscle mRNA expression of inflammatory cytokine genes *TNF-α, IFN-γ, IL-6,* and *IL-1ß* were markedly increased in SIV-infected animals (Figure 1). *IL-6* mRNA expression was significantly greater in the SIV-infected animals ($P < .05$) (Figure 1). A trend of higher expression of all inflammatory cytokines was observed in skeletal muscle of ALC/SIV$^+$ animals. However, this trend did not reach statistical significance. Only *IL-6* and *IL-1ß* mRNA expression was detected in skeletal muscle obtained from control animals. Skeletal muscle antioxidant capacity was significantly reduced in SUC/SIV$^+$ animals by 2.5-fold ($P < .05$) and in ALC/SIV$^+$ animals by ∼7-fold ($P < .01$) (Figure 1).

SIV Infection and Chronic Binge Alcohol Consumption Disrupt Anabolic Signaling Pathways

Insulin-receptor signaling cascade proteins and downstream targets were assessed by Western blot analysis. There were no statistical differences in the protein content of IRS-1, IRS-2, IRβ, PI3-K, Akt1, Akt2, and GLUT4 between groups (Figure 2). The PTP1B protein content was not altered by SIV infection but was significantly increased in the ALC/SIV$^+$ animals ($P < .01$)

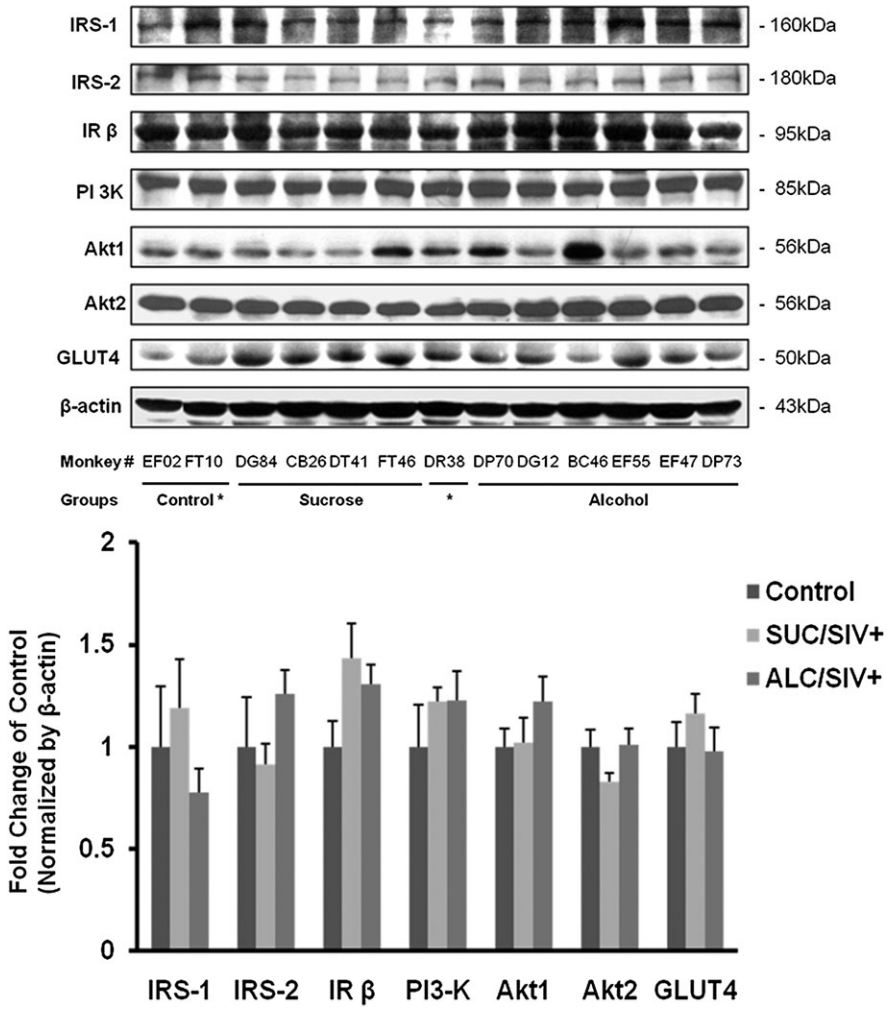

Figure 2. Skeletal muscle insulin signaling pathway protein expression. Protein expression of members of the insulin signaling pathway (insulin receptor substrate 1 [IRS-1], insulin receptor substrate 2 [IRS-2], and insulin receptor β subunit [IRβ]) and downstream targets (Akt1, Akt2, and glucose transporter type 4 [GLUT4]) in skeletal muscle of control animals (n = 8), sucrose-treated simian immunodeficiency virus (SIV)–infected (SUC/SIV$^+$) animals (n = 9), and chronic binge alcohol-administered SIV-infected (ALC/SIV$^+$) animals (n = 11). Shown are representative Western blot images and below mean (± SEM) densitometry values. Expression was normalized to ß-actin and expressed as fold change of control values. There were no statistical differences in variables analyzed using 1-way analysis of variance with a Kruskal-Wallis test followed by a Dunn multiple comparisons test.

(Figure 3). However, overall skeletal muscle PTP1B activity did not differ between groups (Figure 3). IRS-1–associated PI3-K activity was not changed by SIV infection but was significantly reduced in skeletal muscle of ALC/SIV$^+$ animals ($P < .05$) (Figure 4). Expression of *mTOR* mRNA was significantly reduced in skeletal muscle of both SUC/SIV$^+$ and ALC/SIV$^+$ animals ($P < .05$) (Figure 4). In contrast, *atrogin-1* mRNA expression was markedly increased in skeletal muscle from both SIV-infected groups ($P < .01$) (Figure 4).

SIV Infection and Chronic Binge Alcohol Consumption Alter Protein Expression of Ub-Proteasome System Components and Increase Proteasome Activity

SIV infection did not affect skeletal muscle expression of the 20S catalytic core (β21) of the 26S proteasome (Figure 5). However, SIV infection increased protein expression of the 19S base (S5A subunit) in both sucrose-administered macaques ($P < .05$) and alcohol-administered macaques ($P < .01$), but it did not produce significant alterations in protein expression of 19S lid subunits Rpn6 and Rpn12 (Figure 5). In skeletal muscle of ALC/SIV$^+$ macaques an additional marked increase in protein expression of both Rpn6 and Rpn12 was observed ($P < .01$) (Figure 5). Proteasome activity in skeletal muscle isolated from SIV-infected animals did not reflect any significant changes (Figure 5). However, when stratified by time after SIV infection, skeletal muscle obtained from the late infection ALC/SIV$^+$ group showed significant increases in 20S proteasome activity compared with the late infection SUC/SIV$^+$ group ($P < .05$) (Figure 5).

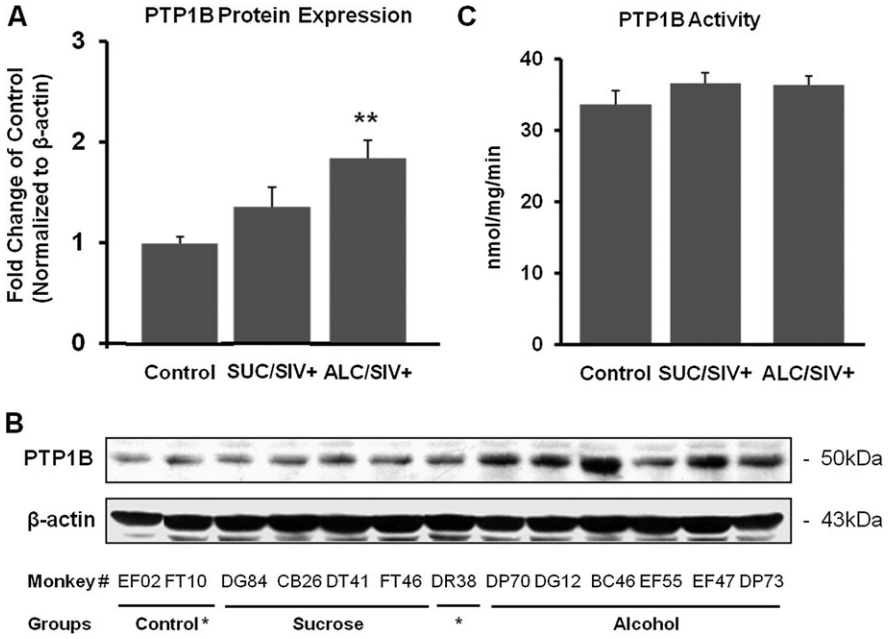

Figure 3. Skeletal muscle protein-tyrosine phosphatase 1B (PTP1B) protein expression and activity. *A,* PTP1B protein expression in skeletal muscle of control animals (n = 8), sucrose-treated simian immunodeficiency virus (SIV)–infected (SUC/SIV$^+$) animals (n = 9), and chronic binge alcohol-administered SIV-infected (ALC/SIV$^+$) animals (n = 11). Expression was normalized to ß-actin and expressed as fold change of control values. *B,* Representative PTP1B Western blot images. *C,* PTP1B activity in skeletal muscle of control animals (*n* = 8), SUC/SIV$^+$ animals (n = 7), and ALC/SIV$^+$ animals (n = 11). *P* values were obtained using 1-way analysis of variance with a Kruskal-Wallis test followed by a Dunn multiple comparisons test. $^{**}P < .01$ versus control.

DISCUSSION

The present study examined the impact of chronic binge alcohol intake on anabolic and catabolic mechanisms of muscle wasting in SIV-infected rhesus macaques. SIV infection created an inflammatory and oxidative milieu in skeletal muscle. These changes were associated with increased *atrogin-1* and decreased *mTOR* mRNA expression. Chronic binge alcohol augmented skeletal muscle oxidative stress, dysregulated Ub-proteasome system subunit expression, and increased proteasome activity in late infection animals. Moreover, chronic binge alcohol increased PTP1B protein expression, and decreased IRS-1–associated PI3-K activity in SIV-infected macaques. Interestingly, in previous studies chronic binge alcohol for up to 13 months in uninfected macaques failed to alter skeletal muscle mRNA expression of *IL-6, TNF-α,* and *atrogin-1* [25]. Taken together, these findings suggest that alcohol amplifies catabolic and blunts anabolic skeletal muscle mechanisms in SIV-infected macaques, contributing to muscle wasting.

Previously we demonstrated that SUC/SIV$^+$ animals did not show significant alterations in BMI, although the observed BMI in ALC/SIV$^+$ animals was 20% lower in animals with SAIDS [18]. In addition, our studies demonstrated that ALC/SIV$^+$ macaques had significantly lower limb muscle area compared with SUC/SIV$^+$ macaques with SAIDS [18]. Moreover, limb, abdominal, and hip circumferences were all 5%–10% smaller in ALC/SIV$^+$ animals, but skinfolds were not significantly smaller. These findings suggested that these changes were not due to loss of subcutaneous fat but due to loss in muscle mass [18]. Weight loss, particularly loss of metabolically active lean tissue, has been associated with accelerated disease progression, loss of muscle protein mass, and impairment of strength and functional status in HIV-infected individuals [30]. The findings from the present study provide insight into the mechanisms responsible for the greater loss in skeletal muscle. Contrary to what we expected, with the exception of proteasome activity, the derangements in skeletal muscle components of both anabolic and catabolic pathways were already evident during the first 10 months of infection. These findings suggest that changes in the skeletal muscle milieu leading to muscle wasting in SIV infection occurs throughout the course of infection and is possibly enhanced as the disease progresses.

Previous studies in patients with AIDS wasting have provided evidence for the involvement of the Ub-proteasome system in loss of skeletal muscle mass, and it has been suggested that this pathway is activated by pro-inflammatory cytokines such as TNF-α and glucocorticoids, leading to AIDS-associated wasting [31]. Mild oxidative stress causes increased protein catabolism and increased expression of Ub-proteasome system components in skeletal myotubes [32]. Oxidative stress also increases muscle-specific E2 and E3 proteins (enzymes involved in activating and attaching ubiquitin to substrates for degradation by the 26S

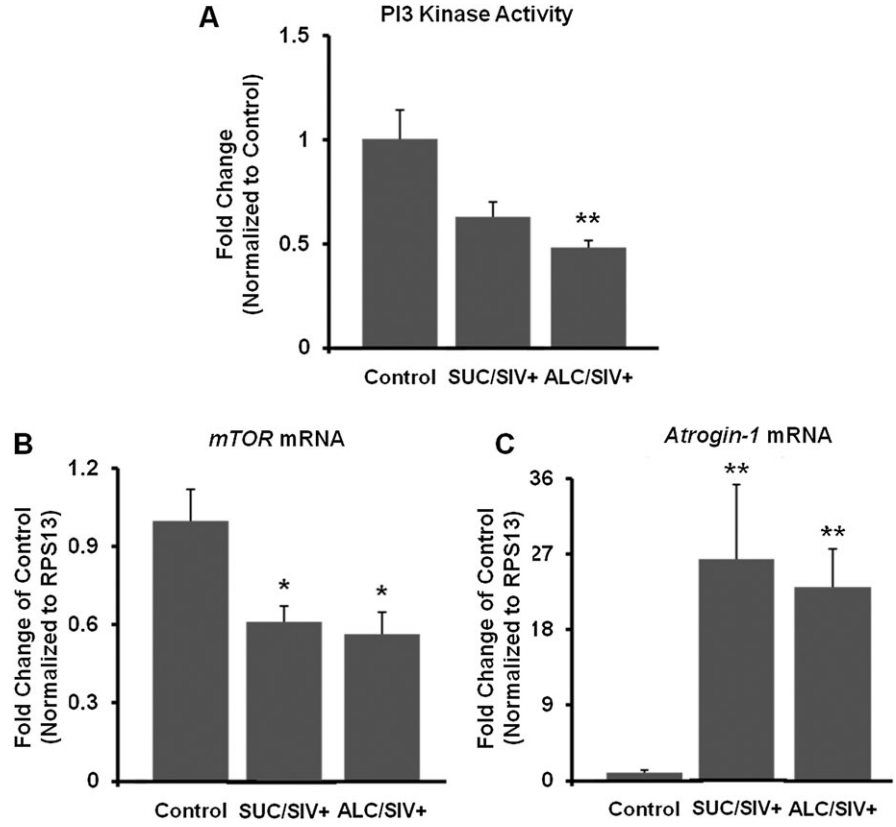

Figure 4. Skeletal muscle phosphatidylinositol 3 kinase (PI3-K) activity, mTOR expression, and atrogin 1 expression. *A,* PI3-K activity normalized to levels in control animals (n = 8) in sucrose-treated simian immunodeficiency virus (SIV)–infected (SUC/SIV$^+$) animals (n = 9) and chronic binge alcohol-administered SIV-infected (ALC/SIV$^+$) animals (n = 11). *B, C,* Levels of *mTOR* gene and *atrogin-1* gene messenger RNA (mRNA) expression, respectively, expressed as fold change of control values (n = 5) in SUC/SIV$^+$ (n = 9) animals and ALC/SIV$^+$ animals (n = 10). *P* values were obtained using 1-way analysis of variance with a Kruskal-Wallis test followed by a Dunn multiple comparisons test. *$P < .05$ versus control; **$P < .01$ versus control.

proteasome) that regulate muscle catabolism [33]. The 26S proteasome is responsible for the degradation of intracellular proteins and is composed of a 20S catalytic core and 19S polar caps. The 19S caps are made up of a lid and a base composed of several regulatory protein subunits. The results from the present study support those findings. A lower antioxidant capacity was observed in skeletal muscle of ALC/SIV$^+$ animals, which was associated with increased protein expression of the 19S base (S5A). Although SUC/SIV$^+$ animals showed no change in measured Rpn subunit expression, ALC/SIV$^+$ animals had significantly increased protein expression of Rpn6 and Rpn12. The function of the Rpn subunits is not completely understood. However, studies report that Rpn6 is essential for the proper assembly of the 19S lid component as well as the proper functioning of the 26S proteasome [34].

We have previously shown that skeletal muscle *IGF-1* mRNA expression is decreased in both SUC/SIV$^+$ and ALC/SIV$^+$ animals with SAIDS, suggesting suppression of anabolic regulation of skeletal muscle mass [18]. The results of the present study provide further support for that hypothesis. Our results show that the protein content of a specific phosphatase, PTP1B, is significantly increased in ALC/SIV$^+$ macaques. PTP1B is a negative regulator of cellular insulin signaling and is responsible for insulin receptor dephosphorylation, resulting in termination of insulin signaling. PTP1B also dephosphorylates IRS-1, resulting in deactivation of this insulin signaling mediator [35]. Additionally, PTP1B has been shown to regulate IGF-1 receptor kinase activity, and upregulation of PTP1B decreased both IGF-1 receptor and Akt activation [36]. Thus, we predict that increased expression PTP1B results in impaired insulin- and IGF-1–mediated anabolic effects, and that this is further enhanced in ALC/SIV$^+$ animals.

In parallel, our results show that PI3-K activity is significantly decreased in skeletal muscle of ALC/SIV$^+$ animals. This may be due to increased PTP1B expression decreasing insulin and IGF-1 signaling. Decreased PI3-K activity would be expected to result in decreased Akt activation and consequently decreased mTOR and forkhead box (FoxO) phosphorylation, as illustrated in Figure 6. Both mTOR and FoxO are important transcription factors involved in muscle anabolic and catabolic responses through their modulation of protein synthesis (mTOR) and muscle-specific E3 ligase (*atrogin-1* and *MuRF-1*) gene expression. When FoxO

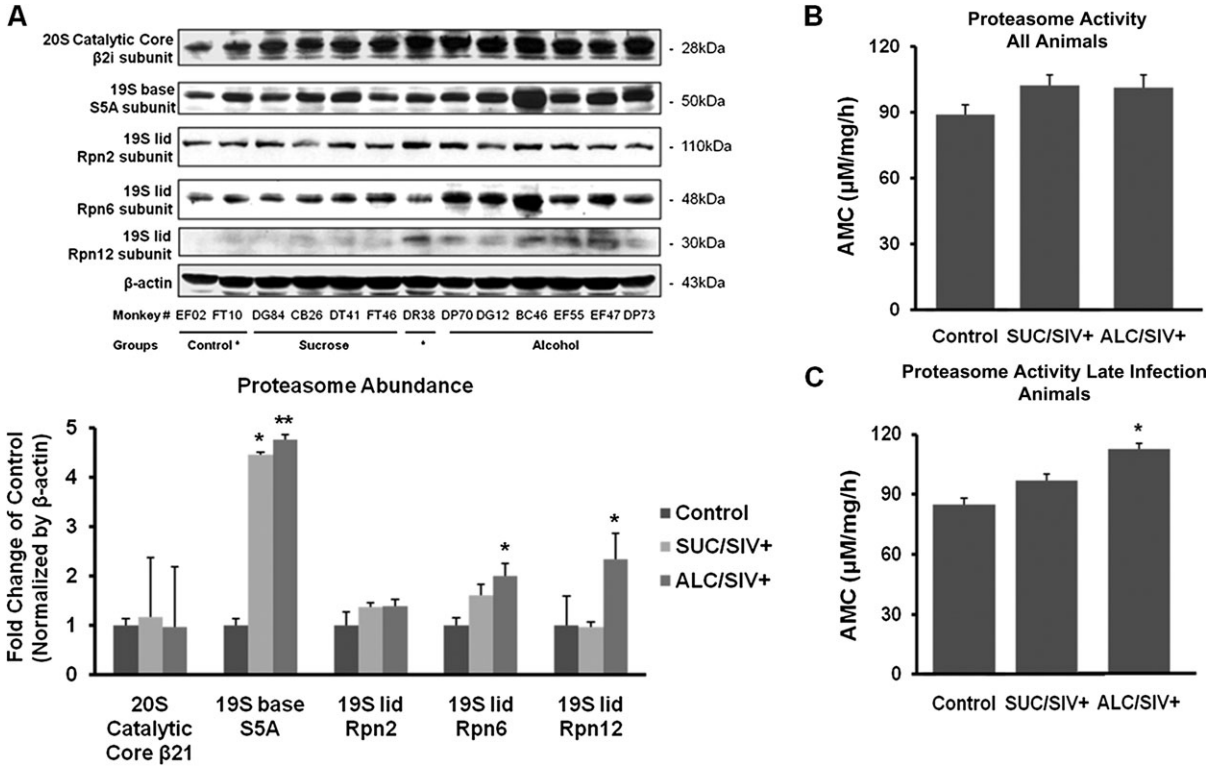

Figure 5. Skeletal muscle Ub-proteasome system subunit expression and proteasome activity. *A,* Representative Western blot and mean (± SEM) densitometric values of proteasome subunit expression in skeletal muscle of control animals (n = 8), sucrose-treated simian immunodeficiency virus (SIV)–infected (SUC/SIV$^+$) animals (n = 9), and chronic binge alcohol-administered SIV-infected (ALC/SIV$^+$) animals (n = 11). Expression was normalized to ß-actin and expressed as fold change of control values. *B,* Proteasome activity in skeletal muscle of control animals (n = 8), SUC/SIV$^+$ animals (*n* = 9), and ALC/SIV$^+$ animals (n = 11). *C,* Proteasome activity in control (n = 8) and late infection animals, SUC/SIV$^+$ animals (n = 3), and ALC/SIV$^+$ animals (n = 3). *P* values were obtained by 1-way analysis of variance with a Kruskal-Wallis test followed by a Dunn multiple comparisons test. $*P < .05$ versus control; $**P < .01$ versus control. AMC, 7-amino-4-methylcoumarin.

proteins are phosphorylated they are unable to translocate to the nucleus and promote transcription of the E3 ligases. These muscle-specific ubiquitin ligases target muscle proteins for degradation by the Ub-proteasome system. We speculate that decreased PI3-K activity leads to decreased Akt-mediated phosphorylation of mTOR and FoxO family members (Figure 6). Our results show significantly decreased *mTOR* and increased *atrogin-1* mRNA expression in skeletal muscle of SIV-infected

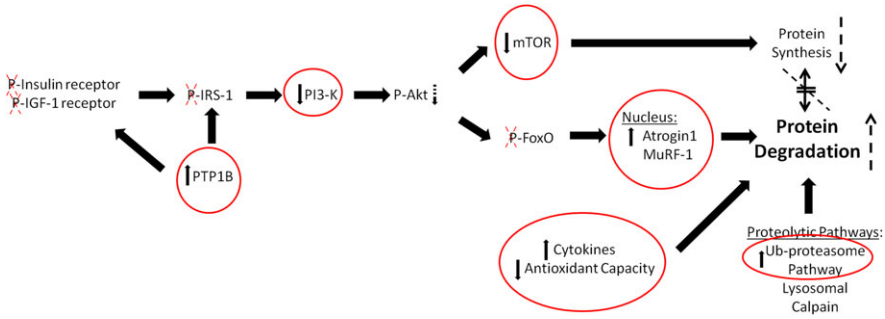

Figure 6. Pathways involved in protein turnover. Protein turnover involves a delicate balance of synthetic and catabolic mechanisms. Insulin and insulin-like growth factor 1 (IGF-1) signaling lead to protein synthesis through activation of the mTOR pathway, Akt signaling, and phosphorylation of forkhead box (FoxO). Protein degradation occurs via major cellular proteolytic pathways, which can be enhanced by cytokines and reactive oxygen species. Dysregulated insulin signaling, increased cytokine expression, decreased antioxidant capacity, and upregulation of the Ub-proteasome system can all lead to an imbalance in protein turnover, favoring degradation over synthesis. Circled pathway members, with arrows indicating direction of change, are the results presented in this article. Dashed arrows and crosses show what we predict occurs to other pathway members based on the data we have presented. Together, these changes may lead to decreased protein synthesis and enhanced protein breakdown.

animals. In another study, we found that *MuRF-1* mRNA levels were increased in both SUC/SIV$^+$ and ALC/SIV$^+$ animals with SAIDS [18].

Taken together, the results of our studies demonstrate that chronic alcohol consumption during SIV infection may lead to decreased insulin anabolic regulation of skeletal muscle mass, as reflected by the increased PTP1B expression, decreased PI3-K activity, reduced *mTOR* expression, and increased muscle-specific E3 ubiquitin ligase expression (Figure 6). We propose that this dysfunctional insulin signaling is a mechanism that likely contributes to SIV- and HIV-associated muscle wasting. Thus, these findings suggest that the decrease in muscle mass in animals with SAIDS is likely the result of a combination of a pro-inflammatory, pro-oxidative, and anabolic imbalance that favors catabolic processes leading to loss of muscle mass and impaired muscle growth. These findings are in agreement with previous reports in the literature from clinical studies indicating that inflammation impacts the responsiveness of muscle tissue to an anabolic stimulus [37] and is associated with marked alterations of protein metabolism [38, 39].

In conclusion, our results show that SIV infection results in marked alterations in the skeletal muscle milieu that are characterized by inflammation and oxidative stress. These are associated with significant derangements in components of catabolic and anabolic pathways responsible for maintenance of skeletal muscle mass. In addition, we show that chronic alcohol accentuates the pro-oxidative and pro-inflammatory skeletal muscle milieu, further disrupting both anabolic and catabolic regulatory mechanisms and promoting loss of skeletal muscle mass. In combination, the altered signaling mechanisms and inflammatory and oxidative milieu are likely central mechanisms for the accentuated SAIDS wasting of chronic binge alcohol-treated SIV-infected animals previously reported by our laboratory.

Notes

Acknowledgments. We acknowledge the technical expertise of Jean Carnal, Curtis Vande Stouwe, and Meredith Booth. We also thank Peter Didier for providing the control macaque muscle samples and Robert Siggins for his careful review of this manuscript.

Financial support. This work was supported by the National Institute on Alcohol Abuse and Alcoholism, National Institutes of Health (NIH) (AA07577, AA09803, and AA11290); and National Institute of Diabetes and Digestive and Kidney Diseases, NIH (DK072909).

Potential conflicts of interest. All authors: No reported conflicts.

All authors have submitted the ICMJE Form for Disclosure of Potential Conflicts of Interest. Conflicts that the editors consider relevant to the content of the manuscript have been disclosed.

References

1. CDC. HIV/AIDS Surveillance Report. Vol 15. Atlanta: US Department of Health and Human Services, CDC, **2003**.
2. Lefevre F, O'Leary B, Moran M, et al. Alcohol consumption among HIV-infected patients. J Gen Intern Med **1995**; 10:458–60.
3. Lee LM, Karon JM, Selik R, Neal JJ, Fleming PL. Survival after AIDS diagnosis in adolescents and adults during the treatment era, United States, 1984–1997. JAMA **2001**; 285:1308–15.
4. Grunfeld C, Feingold KR. Metabolic disturbances and wasting in the acquired immunodeficiency syndrome. N Engl J Med **1992**; 327:329–37.
5. Van Loan MD, Strawford A, Jacob M, Hellerstein M. Monitoring changes in fat-free mass in HIV-positive men with hypotestosteronemia and AIDS wasting syndrome treated with gonadal hormone replacement therapy. AIDS **1999**; 13:241–8.
6. Wanke CA, Silva M, Knox TA, Forrester J, Speigelman D, Gorbach SL. Weight loss and wasting remain common complications in individuals infected with human immunodeficiency virus in the era of highly active antiretroviral therapy. Clin Infect Dis **2000**; 31:803–5.
7. Tang AM, Forrester J, Spiegelman D, Knox TA, Tchetgen E, Gorbach SL. Weight loss and survival in HIV-positive patients in the era of highly active antiretroviral therapy. J Acquir Immune Defic Syndr **2002**; 31:230–6.
8. Preedy VR, Salisbury JR, Peters TJ. Alcoholic muscle disease: features and mechanisms. J Pathol **1994**; 173:309–15.
9. Reilly ME, Mantle D, Richardson PJ, et al. Studies on the time-course of ethanol's acute effects on skeletal muscle protein synthesis: comparison with acute changes in proteolytic activity. Alcohol Clin Exp Res **1997**; 21:792–8.
10. Pacy PJ, Preedy VR, Peters TJ, Read M, Halliday D. The effect of chronic alcohol ingestion on whole body and muscle protein synthesis—a stable isotope study. Alcohol Alcohol **1991**; 26:505–13.
11. Lang CH, Wu D, Frost RA, Jefferson LS, Kimball SR, Vary TC. Inhibition of muscle protein synthesis by alcohol is associated with modulation of eIF2B and eIF4E. Am J Physiol **1999**; 277:E268–76.
12. Teschner M, Schaefer RM, Weissinger F, et al. Chronic ethanol ingestion enhances catabolism and muscle protease activity in acutely uremic rats. Nephron **1988**; 50:338–44.
13. Molina PE, Fan J, Gelato M, Lang CH, Abumrad NN. Modulation of insulin-like growth factor-I: a specific role for vitamin B1 (thiamine). J Nutr Biochem **1996**; 7:207–13.
14. Suttmann U, Ockenga J, Selberg O, Hoogestraat L, Deicher H, Muller MJ. Incidence and prognostic value of malnutrition and wasting in human immunodeficiency virus-infected outpatients. J Acquir Immune Defic Syndr Hum Retrovirol **1995**; 8:239–46.
15. Wheeler DA, Gibert CL, Launer CA, et al. Weight loss as a predictor of survival and disease progression in HIV infection. Terry Beirn Community Programs for Clinical Research on AIDS. J Acquir Immune Defic Syndr Hum Retrovirol **1998**; 18:80–5.
16. Thiebaut R, Malvy D, Marimoutou C, Davis F. Anthropometric indices as predictors of survival in AIDS adults: Aquitaine Cohort, France, 1985–1997. Groupe d'Epidemiologie Clinique du Sida en Aquitaine (GECSA). Eur J Epidemiol **2000**; 16:633–9.
17. Coodley GO, Loveless MO, Merrill TM. The HIV wasting syndrome: a review. J Acquir Immune Defic Syndr **1994**; 7:681–94.
18. Molina PE, Lang CH, McNurlan M, Bagby GJ, Nelson S. Chronic alcohol accentuates simian acquired immunodeficiency syndrome-associated wasting. Alcohol Clin Exp Res **2008**; 32:138–47.
19. Attaix D, Ventadour S, Codran A, Bechet D, Taillandier D, Combaret L. The ubiquitin-proteasome system and skeletal muscle wasting. Essays Biochem **2005**; 41:173–86.
20. de Alvaro C, Teruel T, Hernandez R, Lorenzo M. Tumor necrosis factor alpha produces insulin resistance in skeletal muscle by activation of inhibitor kappaB kinase in a p38 MAPK-dependent manner. J Biol Chem **2004**; 279:17070–8.
21. Nieto-Vazquez I, Fernandez-Veledo S, Kramer DK, Vila-Bedmar R, Garcia-Guerra L, Lorenzo M. Insulin resistance associated to obesity: the link TNF-alpha. Arch Physiol Biochem **2008**; 114:183–94.
22. Thomas M, Langley B, Berry C, et al. Myostatin, a negative regulator of muscle growth, functions by inhibiting myoblast proliferation. J Biol Chem **2000**; 275:40235–43.
23. Gonzalez-Cadavid NF, Taylor WE, Yarasheski K, et al. Organization of the human myostatin gene and expression in healthy men and HIV-infected men with muscle wasting. Proc Natl Acad Sci U S A **1998**; 95:14938–43.

24. Bagby GJ, Stoltz DA, Zhang P, et al. The effect of chronic binge ethanol consumption on the primary stage of SIV infection in rhesus macaques. Alcohol Clin Exp Res **2003**; 27:495–502.
25. Molina PE, McNurlan M, Rathmacher J, et al. Chronic alcohol accentuates nutritional, metabolic, and immune alterations during asymptomatic simian immunodeficiency virus infection. Alcohol Clin Exp Res **2006**; 30:2065–78.
26. de Jonge HJ, Fehrmann RS, de Bont ES, et al. Evidence based selection of housekeeping genes. PLoS One **2007**; 2:e898.
27. Klemm A, Voigt C, Friedrich M, et al. Determination of erythrocyte antioxidant capacity in haemodialysis patients using electron paramagnetic resonance. Nephrol Dial Transplant **2001**; 16:2166–71.
28. Wang ZQ, Floyd ZE, Qin J, et al. Modulation of skeletal muscle insulin signaling with chronic caloric restriction in cynomolgus monkeys. Diabetes **2009**; 58:1488–98.
29. Wang ZQ, Ribnicky D, Zhang XH, et al. An extract of *Artemisia dracunculus* L. enhances insulin receptor signaling and modulates gene expression in skeletal muscle in KK-A(y) mice. J Nutr Biochem **2011**; 22:71–8.
30. Mangili A, Murman DH, Zampini AM, Wanke CA. Nutrition and HIV infection: review of weight loss and wasting in the era of highly active antiretroviral therapy from the nutrition for healthy living cohort. Clin Infect Dis **2006**; 42:836–42.
31. Llovera M, Garcia-Martinez C, Agell N, et al. Ubiquitin and proteasome gene expression is increased in skeletal muscle of slim AIDS patients. Int J Mol Med **1998**; 2:69–73.
32. Gomes-Marcondes MC, Tisdale MJ. Induction of protein catabolism and the ubiquitin-proteasome pathway by mild oxidative stress. Cancer Lett **2002**; 180:69–74.
33. Li YP, Chen Y, Li AS, Reid MB. Hydrogen peroxide stimulates ubiquitin-conjugating activity and expression of genes for specific E2 and E3 proteins in skeletal muscle myotubes. Am J Physiol Cell Physiol **2003**; 285:C806–12.
34. Isono E, Saito N, Kamata N, Saeki Y, Toh-E A. Functional analysis of Rpn6p, a lid component of the 26 S proteasome, using temperature-sensitive rpn6 mutants of the yeast *Saccharomyces cerevisiae*. J Biol Chem **2005**; 280:6537–47.
35. Goldstein BJ, Bittner-Kowalczyk A, White MF, Harbeck M. Tyrosine dephosphorylation and deactivation of insulin receptor substrate-1 by protein-tyrosine phosphatase 1B: possible facilitation by the formation of a ternary complex with the Grb2 adaptor protein. J Biol Chem **2000**; 275:4283–9.
36. Buckley DA, Cheng A, Kiely PA, Tremblay ML, O'Connor R. Regulation of insulin-like growth factor type I (IGF-I) receptor kinase activity by protein tyrosine phosphatase 1B (PTP-1B) and enhanced IGF-I-mediated suppression of apoptosis and motility in PTP-1B-deficient fibroblasts. Mol Cell Biol **2002**; 22:1998–2010.
37. Gelato MC, Mynarcik D, McNurlan MA. Soluble tumour necrosis factor alpha receptor 2, a serum marker of resistance to the anabolic actions of growth hormone in subjects with HIV disease. Clin Sci (Lond) **2002**; 102:85–90.
38. Lang CH, Silvis C, Deshpande N, Nystrom G, Frost RA. Endotoxin stimulates in vivo expression of inflammatory cytokines tumor necrosis factor alpha, interleukin-1beta, -6, and high-mobility-group protein-1 in skeletal muscle. Shock **2003**; 19:538–46.
39. Frost RA, Lang CH. Skeletal muscle cytokines: regulation by pathogen-associated molecules and catabolic hormones. Curr Opin Clin Nutr Metab Care **2005**; 8:255–63.